Advanced Embedding Technique For Improving Resolution Using Speed Tensor Algorithm

Mekala Ganesh Kumar[1], T.Bathina Babu[2], B.Ramesh Naik[3]

[1, 2, 3] Department of ECE

[1, 2, 3] Seshachala Institute of Technology, Puttur , AP, INDIA.

Abstract- *Neighbors embedding (NE) technology has proved its efficiency in single image tremendous resolution (SITR). However, picture patches do not strictly comply with the identical structure within the low-resolution and excessive-decision areas, accordingly leading to a bias to the snapshot restoration. In this paper, considering that patches are a collection of knowledge with multiview characteristics and spatial organization, we increase a twin-geometric neighbor embedding method for SITR. In this Method, multiview features and local spatial neighbors of patches are explored to discover a function-spatial manifold embedding for pictures. We undertake a geometrically motivated assumption that for each patch there exists a small nearby in which handiest the patches that come from the same feature-spatial manifold, will lie roughly in a low-dimensional affine subspace formulated by using sparse neighbors. With a purpose to find the sparse neighbors, a tensorsimultaneous orthogonal matching pursuit algorithm is developed to fully grasp a joint sparse coding of feature-spatial image tensors. Some experiments are performed on realizing a 3X amplification of average pics, and the recovered results show its effectivity and superiority to its counterparts.*

I. INTRODUCTION

Within the final decade, there have increasing interests in synthesizing a brand new high-Rresolution (HR) image with the aid of making use of one Low-resolution (LR) picture and a set of examples [1], including okay-nearest neighbors synthesis algorithms [2]–[6], sparse coding algorithms [7]–[11], sparse regression algorithms [12]–[14], self-similarity finding out algorithms [15]–[19], and so on. One of the crucial representative works is the Neighbors Embedding (NE) method [4] that generates HR patches through locally Linear Embedding (LLE) [20]. LLE is a famous manifold finding out approach whose purpose is to find a low-dimensional embedding that first-class preserves the local geometry of information.
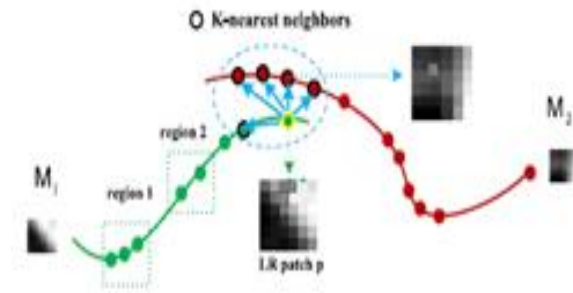

Fig.1. Manifolds close to each other and have arbitrary dimensions and   curvature.

Each datum is assumed to be linearly represented by its k nearest neighbors in a local region, and the low-dimensional embedding is calculated by the nearest neighbors and their weights [20]. In Chang's method [4], the authors assumed that LR patches and HR patches form manifolds with similar local geometry in two distinct spaces. Then LLE is introduced to estimate HR patches by weightedly combining k candidate HR patches selected from the training examples. Compare to the traditional interpolation-based Single Image Super-Resolution (SISR) approaches, the NE-based SISR method and its variants have shown better generalization capability for a variety of images [4]–[6], [21]–[25]. The preservation of local geometry of data in the embedding space is very challenging for the inherent ill-posed characteristic of SISR. Most of available NE-based SISR methods [4]–[6] believe that using first-order and second-order gradients as LR features can better preserve the local geometry of HR patches.

However, patches from real-world images are so diverse that patches will lie in multiple manifolds or subspaces of possibly different dimensions, and consequently manifolds may be very close to each other and have arbitrary dimensions and curvature [9], [11]–[13], [16], [25]. Therefore, image patches do not strictly follow the similar structure in a single LR feature space and HR image space, which leads to an inaccurate LLE and a bias to the image restoration. Fig.1 depicts the mismatch of manifold structure of image patches in the LR-to-HR mapping. Some works have been proposed to overcome the mismatch of manifold structure of image patches in the LR-to-HR mapping. For example, paper [26] presented a projection matrix learning approach to preserve the intrinsic geometric manifold structure of HR image

patches, by using a locally smooth constraint as a prior knowledge of reconstruction. Paper [27] proposed an improved embedding method for face hallucination by incorporating the position prior of face and local geometry of HR patch manifold, but it is limited by the position prior of face, so it could not be directly transferred to natural images.
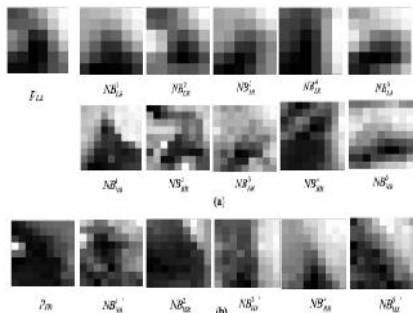

Fig. 2. Demonstration of the deviation of in the neighborhood neighbor embedding.
(a) PSNR = 20.37 dB. (b) PSNR = 29.Forty dB

It's good known that the randomly generated image patches are so numerous that they will lie in more than one manifolds [9], [11]–[13], [16], [25]. If the manifolds are close to every other, equivalent to two manifolds M1 and M2 in Fig.1, then the k nearest neighbors of an image patch p belongs to M1, will come from a further manifold, M2. When k nearest neighbors are used to synthesize the HR patch, it's going to lead to an apparent bias to there construction, due to the fact that handiest the neighbors in M1 span a 1D subspace around the patch [28]. Fig.2(a) shows an LR snapshot patch pLR and its 5 neighbors NB1 LR, . . . NB5 LR discovered by the first-order and 2nd-order gradients in Chang's procedure, and the 2d line indicates the five corresponding HR patches of the LR neighbors. Fig.2(b) suggests the HR picture patch and its five neighbors NB1 HR, . . . NB5 HR discovered within the HR area, additionally, the PSNR via making use of HR neighbors from (a) and (b) respectively are culculated, from which we can see that the five HR neighbors in Fig.2(a) and Fig.2(b) are very various, which verifies the inconsistency of the manifold constitution in an LR-HR mapping. With a view to overcome this mismatch of manifold structure, many changes on NE-based SISR approaches had been proposed, which can be classified into two classes.

A. Elevated Neighbors Embedding and Neighbor choice:

Su et al. [21] addressed the local predicament in SISR and indicated that the illuminance price can better expose the manifold constitution of HR patches. Fan et al. [22] advanced an effective learnt picture primitive mannequin by way of examining the local structure in a Mid-frequency (MF)-to-excessive-frequency (HF) mapping. In [23], Chan et

al. Used characteristic selection to reinforce the recovery accuracy of LR patches. In very contemporary works, coupled constraints centered joint finding out is advanced for higher embedding [16], and an adaptive sparse embedding is provided in [24].

B. Subtle training knowledge Set:

Several works used the sophisticated coaching patches to make the manifolds comply with the an identical structure. For example, in [25] the authors designed a HoG function-established subset determination to refine the dataset with the aid of deleting some outlier patches, which works well on typical photos. In [23], the training patches are refined by way of aspect detection, and in [24] clustering algorithm is used to predict category label within the neighbor search, where the coaching patches are divided into exclusive corporations and only one crew is adopted for finding an embedding. Although many efforts were taken on finding the superior embedding manifolds and neighbors in these works, two issues will have to be addressed for making improvements to to be had NE-founded SISR strategies:

1) Pix Patches Have Multiview and Heterogeneous Representations: it's good recognized that partial representation of patches most effective makes it possible for discovering neighbors in a exact kind of LR characteristic area, where photograph patches don't strictly follow the identical constitution to that of HR patches [9], [11]–[13]. In many real-world eventualities, each object can also be described via a couple of units of elements, where each characteristic describes a view of the Same set of underlying objects. One function that summarizes

A patch can also be regarded as a view of the image patch, and finding multiview illustration that describes the patch persona heterogeneously and integrating them right into a unified illustration for subsequent processing, is a promising manufacturer in snapshot processing [29]. Accordingly, a complete and mutliview representation of patches will aid to raised expose the underlying manifold structure. With a view to to find better embedding manifold, the complementary information of designated features may also be well explored, to reveal special bodily meanings and statistical residences of patches.

2) Pics Patches Are a collection of information With Spatial institution: portraits patches should not best a set of samples but in addition information with some spatial group. Some researchers have indicated that a regional subject in a average image may also be considered as a

stationary process, which will also be well modeled through Autoregressive (AR) items [12]–[13]. There are quite often many repetitive photograph buildings (or self-similarity) in an photograph [15], [16]. When pics are divided into small patches, the patches are self-an identical in a local neighborhood, that's, an image patch is ordinarily just like its neighbor patches headquartered round it [17]–[19]. Hence, these similar patches will Have the similar neighbors within the manifold embedding and neighbor search. Even though this self-an identical attribute has been most often utilized in different SISR approches [15]–[19], it is not often explored in on hand NE situated SISR methods. Summarily, photo patches have inherent geometric structure in both the underlying multiview features area and the spatial area. In order to find a low-dimensional embedding that well preserves the neighborhood geometry of image patches, on this paper we discover this dual-geometric constitution in the featurepatial area, to strengthen a brand new dual-Geometric Neighbor Embedding (DGNE) approach for SISR. In DGNE, multiview facets and nearby spatial neighbors of patches are explored to find a characteristic-spatial manifold embedding for pictures. We use the geometrically motivated assumption that for each and every patch there exists a small regional wherein simplest the patches that come from the identical function-spatial manifold, will lie approximately in a low-dimensional affine subspace. Additionally, the curvature of the manifold and the density of patches could also be unique in unique areas, corresponding to vicinity 1 and neighborhood 2 in M1 in Fig.1. As a consequence patches can be sparsely coded to automatically prefer a few neighbors that span a low-dimensional affine subspace passing close Fig. 3. Multi-view features. (a) Pixel Z33. (b) f1. (c) f2. (d) f3. (e) f4.(f) f5. (g) f6.

Table I

TENSOR- SIMULTANEOUS ORTHOGONAL MATCHING PURSUIT (TENSOR-SOMP) ALGORITHM:

Equal set of underlying objects. One feature that summarizes a patch may also be considered as a view of the photograph patch, and finding multiview illustration that describes the patch personality heterogeneously and integrating them into a unified illustration for subsequent processing, is a promising brand in image processing [29]. As a result, a comprehensive and mutliview representation of patches will support to better reveal the underlying manifold structure. With the intention to in finding higher embedding manifold, the complementary expertise of certain aspects will also be well explored, to reveal distinct bodily meanings and statistical homes of patches. 2) portraits Patches Are a group of data With Spatial group: pix patches will not be best a collection of samplesbut additionally data with some spatial organization. Some researchers have indicated that a nearby area in a average photo will also be seen as a stationary approach, which can also be good modeled via Autoregressive (AR) units [12]–[13]. There are often many repetitive image structures (or self-similarity) in an picture [15], [16]. When pix are divided into small patches, the patches are self-equivalent in a regional region, that's, an snapshot patch is ordinarily similar to its neighbor patches established round it [17]–[19]. For this reason, these equivalent patches will Have the equivalent neighbors within the manifold embedding and neighbor search. Although this self-an identical characteristic has been in most cases utilized in other SISR approches [15]–[19], it is not often explored in to be had NE situated SISR ways. Summarily, photograph patches have inherent

geometric structure in both the underlying multiview features domain and the spatial domain. With a purpose to discover a low-dimensional embedding that well preserves the regional geometry of photo patches, in this paper we explore this twin-geometric structure in the featurepatial area, to boost a brand new twin-Geometric Neighbor Embedding (DGNE) process for SISR. In DGNE, multiview features and regional spatial neighbors of patches are explored to find a feature-spatial manifold embedding for snap shots.

We use the geometrically prompted assumption that for every patch there exists a small nearby where simplest the patches that come from the same feature-spatial manifold, will lie roughly in a low-dimensional affine subspace. In addition, the curvature of the manifold and the density of patches may be exclusive in exclusive regions, akin to area and neighborhood 2 in M1 in Fig.1. As a result patches can be carefully coded to robotically decide on a couple of neighbors that span a low-dimensional affine subspace passing close.
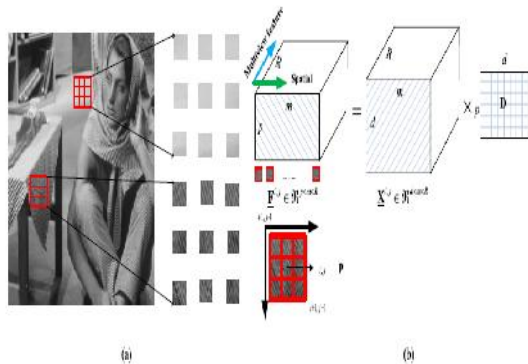

Fig. 4. Exploration of twin-geometric structure of snap shots by way of sparse tensor (a) similarity among the regional eighborhood (b) Sparse coding of characteristic-spatial picture tensor.

II. PROPOSED SYSTEM

In this approach, Image patches have inherent geometric structure in both the underlying multiview features domain and the spatial domain. In order to find a low-dimensional embedding that well preserves the local geometry of image patches, in this paper we explore this dual-geometric structure in the featurepatial domain, to advance a new Dual-Geometric Neighbor Embedding (DGNE) approach for SISR. In DGNE, multiview features and local spatial neighbors of patches are explored to find a feature-spatial manifold embedding for images. We use the geometrically motivated assumption that for each patch there exists a small neighborhood in which only the patches that come from the same feature-spatial manifold, will lie approximately in a low-dimensional affine subspace. Moreover, the curvature of the manifold and the density of patches may be different in

different regions, such as region 1 and region 2 in M1 in Fig.1. Consequently patches can be sparsely coded to automatically select a few neighbors that span a low-dimensional affine subspace passing near the patches, and reveal the intrinsic dimensionality of the underlying manifolds. In our work, considering the existence of the dual-geometry structure in both the feature space and spatial space, LR patches and their spatial neighbors are jointly coded by multiview feature dictionaries. Patches and coding coefficients are represented by a feature-spatial image tensor and a sparse coefficients tensor respectively [30], and a Tensor-Simultaneous Orthogonal Matching Pursuit (T-SOMP) algorithm is advanced for finding the sparse embedding neighbors. Finally some experiments are taken on realizing a 3X amplification of natural images, and the recovered results prove its efficiency and superiority to its counterparts. The remainder of this paper is structured as follows.
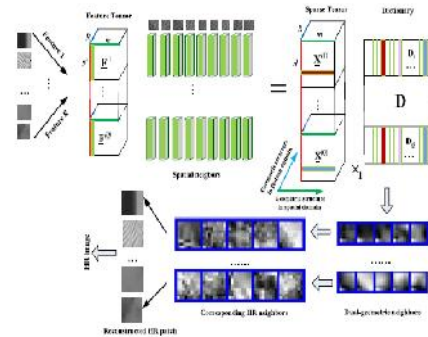
Fig. 5. The framework of the proposed approach

In our work, for the reason that the existence of the twin-geometry structure in each the function space and spatial space, LR patches and their spatial neighbors are collectively coded via multiview function dictionaries. Patches and coding coefficients are represented with the aid of a characteristic-spatial photograph tensor and a sparse coefficients tensor respectively [30], and a Tensor-Simultaneous Orthogonal Matching Pursuit (T-SOMP) algorithm is evolved for locating the sparse embedding neighbors. In the end some experiments are taken on realizing a 3X amplification of ordinary pictures, and the recovered results prove its efficiency and superiority to its counterparts. A. Multiview Features Each image patch can be properly characterized by multiple visual features, and multiple views are present and complementary to each other. A view of patches refers to a type of feature that summarizes a specific characteristic of the data. For instance, Chang's [4] algorithm employed the first-order and second-order gradient as the LR features. Su et al. [21] indicated that gradient features could not reveal the data structure, while the illuminance value of images can better express patches structure. Chan et al. [25] proposed a norm feature for characterizing image patches. In this section, a multiview features set of image patches is defined. For the pixel Z33 in a

5×5 patch in Fig.3 (a), the first set of features is composed by first-order gradients:

f1 = x = Z34 − Z32, f2 = y = Z43 − Z23

Fig 6: Test Images

which describes the variation around the pixel in horizontal and vertical respectively. The second-order gradients of Z33 are defined as,

f3= 2

x =Z35−2Z33+Z31, f4= 2

y =Z53−2Z33+Z13 (2)

Which describes the convex and the concave characteristic around Z33. Additionally, two new features are defined, i.e., Pixel Deviation (PD) and Laplace Gradient (LG) features,

f5 = 9Z33

i=2,3,4 j=2,3,4

Zij,

f6 = 4Z33−Z43−Z23−Z34−Z32 (3)

The two features take the discrepancies of different directions and characteristics of patches into account. So the features can describe the variation of pixels in a local window, and the variation along the cross direction respectively. The PD feature can distinguish smooth patches from patches with textures and edges, and the LG feature can capture the detailed information in the horizontal and vertical directions. The filters that extract these multiview features are shown in Fig.3 (b)-(g). The features of all the pixels in an image patch are vectorized to formulate multiple feature vectors fi (i = 1, . . . , 6) B. Background on Sparse Tensor In the neighbors embedding, the neighbors selection also has a remarkable influence on the embedding result. In the following section we advance a Tensor Simultaneous Orthogonal Matching Pursuit (T-SOMP) algorithm for sparse neighbors selection. So in this section we first make a preparatory introduction on sparse tensors. Given a tensor Y   I1×I2....×IN , its n-mode vectors

are obtained by fixing every index but the one in the mode n [28]. The n-mode unfolding matrix Y(n)   In×I1 I2...In−1 In+1...IN is defined by arranging all the n-mode vectors as columns of a matrix. Then the n-mode product of a tensor with a matrix Z = Y×n A   I1×I2...In−1.×J×In+1...IN is defined by, zi1i2...in−1 j in+1...iN = In in=1yi1i2...iN a j in (4) with ik = 1, 2, . . . , Ik (k = n) and j = 1, 2, . . . , J . In [31], the authors indicated the relationship between the Tucker model and a Kronecker representation. GivenY   I1×I2....×‘IN , y = vec Y and x = vec X, the following two representations are equivalent,

Y = X ×1 D1 ×2 D2.... ×N DN (5)

y = (DN   DN−1   ...   D1) x (6)

where vec Y ≡ vec Y(1)   I I = N n=1 In, i.e., by stacking all the 1-mode vectors [30], [31]. Based on this equivalence, we say that the tensor Y   I1×I2....×IN has a sparse representation with respect to the n-mode dictionaries Dn (n = 1, 2, . . . , N). If its vectorized version admits a k-sparse representation over the Kronecker dictionary D = DN   DN−1   ...   D1, it has an equivalent Tucker representation with a sparse core tensor X, i.e. with only k nonzero entries.

C. Dual-Geometric Neighbor Embedding

With Sparse Tensor Several existing works have indicated that there are often many repetitive image structures (or self-similarity) in an image, especially in a local region [12], [13], [15]–[19]. An example is shown in the Baraba image in Fig.4 (a), where patches in these two regions are similar. Considering this similarity among the local neighbors [32], we define a local neighborhood of patches and construct a dual-geometric neighbor embedding approach for SISR. Assume a √ p× √ p patch p   p centered at the (i, j) –th pixel of the original LR image, and denote the number of multiview features as R. In our method, the multiple features fi (i = 1, . . . , 6) of p and its spatial neighbors are simultaneously used for finding a sparse embedding in the following figures 7,8
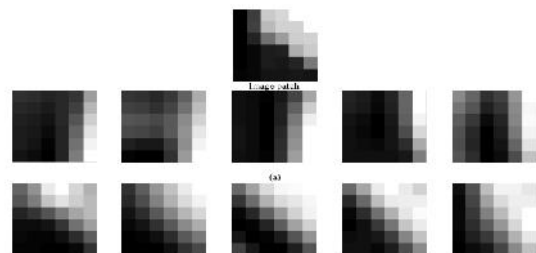

Fig. 7. Neighbors found by multiview features. (a) Neighbors in the first- and second-order gradient feature (f1 & f2 & f3 & f4). (b) Neighbors in themfirst-order gradient and PD feature (f1 & f2 & f3 & f4 & f5).
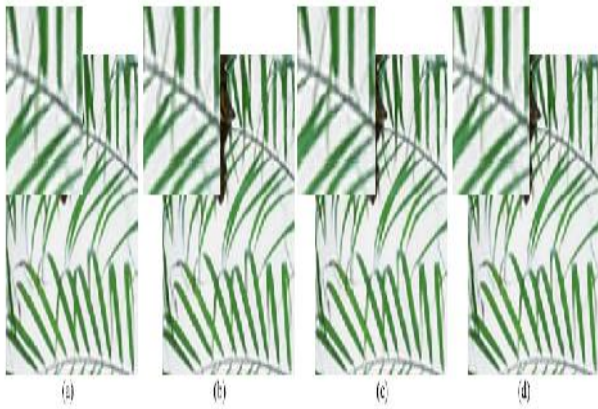
Fig. 8. Reconstructed snap shots with exclusive elements. (a) PSNR = 25.04 dB. (b) PSNR = 25.21 dB. (c) PSNR = 25.Sixteen dB. (d) PSNR = 25.Forty four dB.

An example is shown in the Baraba image in Fig.8, where patches in these two regions are similar. Considering this similarity among the local neighbors [32], we define a local neighborhood of patches and construct a dual-geometric neighbor embedding approach for SISR. Assume a $\sqrt{p} \times \sqrt{p}$ patch p $\;$ p centered at the (i, j) –th pixel of the original LR image, and denote the number of multiview features as R. In our method, the multiple features fi (i = 1, . . . , 6) of p and its spatial neighbors are simultaneously used for finding a sparse embedding.
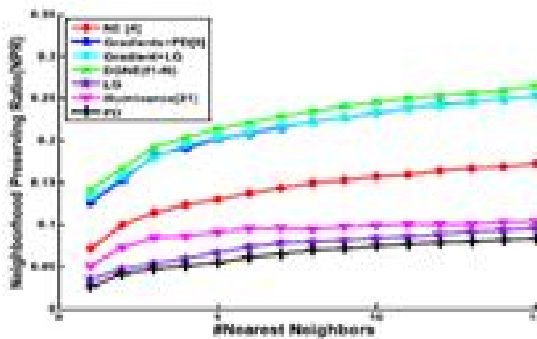

Fig. 9. The Neighborhood preserving ratios of different features.

In the characteristic domain, we first select the closest neighbors subsets FNB1, . . . , FNBR in multiviews area through the Euclidean distance metric. Then these subsets are combined to form a set of candidate neighbors FNB = $\;$ FNBi (|*FNB*| = d) in the feature domain. Similarly in the spatial domain we select the closest neighbors subsets {*SNB*1, . . . , *SNBR*} for *R* views, and form a set of candidate spatial neighbors {*SNB* = $\;$ *SNBi* } (|*SNB*| = m) in the feature domain. This feature-spatial manifold can be analyzed via a tensor form of images. In our method, instead of utilizing vector stacking strategy that simply concatenates different feature vectors, a feature-spatial image tensor is constructed. Because

manifolds may have arbitrary curvature in different regions, we automatically select a few neighbors for patches via tensor sparse representation. For the image patch **p** centered at *(i, j)*, we construct its feature-spatial tensor **F***i, j* $\;$ *_p×m×R*. By casting the sparse prior and dual-geometric constraint on the coding process, we can represent **F***i, j* by a multiview feature dictionary **D***i, j* $\;$ *_p×d* that is composed by the *d* nearest neighbors subsets of the patch **p** centered at *(i, j)*, to obtain the sparse coefficients tensor **X***i, j* $\;$ *_d×m×R*, as shown in Fig.4 (b). According to the Tucker model and Kronecker representation of tensors discussed in section II.B, we have **F***i, j* = **X***i, j* ×**1** **D***i, j* ×**2** **I***m×m* ×**3** **I***R×R* (7) Because very few patches are involved in the sparse coding, **F***i, j* has a sparse representation with respect to the *1*-mode dictionary **D***i, j* *_p×d*. The *1-mode unfolding matrix* can be written as **F***i, j* *(1)* = **D***i, j***X***i, j (1)* *(I*m×m ⊗ **I**R×R) and **vec F***i, j*=*_I*R×R $\;$ **I**m×m ⊗ **D***i, j* $\;$ **vec** *_X*i, j (8) Denote *si, j* as the number of atoms in synthesizing a HR patch for the patch **p**, the number of non-zero elements in **vec X***i, j* is *si, jmR*, i.e., **vec X***i, j* 0 = *si, jmR* << *dmR*. Assuming there are *Q* patches, we can construct a new image tensor **F** $\;$ *_pQ×m×R* and sparse coefficients tensor **X** $\;$ *_dQ×m×R*, which satisfy **F** = **X** ×**1** **D** ×**2** **I***m×m* ×**3** **I***R×R* (9) and **F***(1)* = **DX***(1)* *(I*m×m ⊗ **I**R×R), where **D** = *_D*i, j *_* and there are *si, j* non-zero rows in the *1-mode unfoldingcoefficient matrix* **X***(1)*. Then we solve the sparse tensor **X** via a Tensor-Simultaneous Orthogonal Matching Pursuit (Tensor- SOMP) algorithm, as described in Table I. As soon as **A** is calculated, the sparse tensor **X** can be obtained, from which we can locate the sparse neighbors of the image from its non-zero indexes. Then the atoms in dictionaries are weighted by the sparse coefficients in **X** to recover the HR image. The framework of our proposed method is shown in by which we can understand the whole process more easily. Different with available NE-based SISR methods, the proposed DGNE cannot only combine heterogeneous multiview features together to better reveal the underlying manifold structure, but also jointly code spatial discrepancy patches to derive an accurate dual-geometric neighbors embedding. Moreover, tensor sparse coding will optimize the memory storage and require far fewer iterations compared to the traditional vector-based Orthogonal Matching Pursuit (OMP)

TABLE II

SUMMARY OF PSNR (dB), SSIM AND FSIM RESULTS OF EIGHT TEST IMAGES FOR 3X MAGNIFICATION BY DIFFERENT METHODS. FOR EACH IMAGE, WE HAVE THREE ROWS: PSNR, SSIM AND FSIM

Image	BI	[4]	[11]	[12]	[7]	[13]	SGNE	DGNE
Butter-fly	23.07	25.06	23.93	25.63	27.08	26.78	26.18	**27.06**
	0.787	0.860	0.819	0.884	0.903	**0.904**	0.881	0.890
	0.780	0.863	0.803	0.846	0.884	**0.885**	0.864	0.863
Parrots	27.21	28.47	28.09	27.73	29.48	**30.01**	29.39	29.98
	0.863	0.882	0.881	0.885	0.906	**0.914**	0.902	0.909
	0.902	0.921	0.917	0.921	0.944	**0.944**	0.935	0.940
Bike	22.16	23.22	22.78	23.13	24.34	24.14	23.93	**24.49**
	0.656	0.715	0.702	0.762	0.784	0.793	0.761	**0.793**
	0.768	0.806	0.798	0.825	0.849	**0.859**	0.837	0.854
Flower	26.66	27.75	27.44	27.37	28.76	**29.05**	28.54	29.01
	0.750	0.794	0.787	0.825	0.838	**0.850**	0.826	0.846
	0.825	0.856	0.852	0.848	0.881	**0.895**	0.881	0.887
Girl	32.08	32.56	32.65	31.57	33.07	33.48	33.20	**33.55**
	0.778	0.789	0.798	0.807	0.817	0.823	0.812	**0.827**
	0.867	0.883	0.889	0.882	0.906	0.917	0.906	**0.919**
Hat	28.59	29.98	29.17	29.14	30.97	30.71	30.51	**30.82**
	0.809	0.839	0.827	0.856	0.873	**0.868**	0.854	0.861
	0.836	0.876	0.858	0.880	0.895	**0.905**	0.894	0.900
Leaves	22.35	24.20	23.36	23.81	25.99	26.05	25.44	**26.09**
	0.754	0.844	0.803	0.877	0.892	**0.903**	0.880	0.892
	0.767	0.860	0.800	0.858	0.883	**0.893**	0.871	0.873
Plants	30.22	31.82	31.03	31.34	32.69	33.14	32.56	**33.23**
	0.842	0.879	0.868	0.885	0.902	**0.911**	0.896	0.909
	0.872	0.907	0.892	0.910	0.919	**0.928**	0.918	0.925

TABLE III

RECONSTRUCTED RESULTS OF DGNE WITH DIFFERENT m

m	PSNR(dB)	SSIM	FSIM
9	25.2951	0.8667	0.8956
25	24.3406	0.7845	0.8498
49	22.6782	0.7670	0.8375

Within the feature area, we first choose the closest neighbors subsets FNB1, . . . , FNBR in multiviews area via the Euclidean distance metric. Then these subsets are combined to form a set of candidate neighbors FNB = FNBi FNBin the characteristic area. Similarly in the spatial domain we opt for the closest neighbors subsets SNB1, . . . , SNBR for R views, and kind a set of candidate spatial neighbors SNB = SNBi = m) within the feature domain. This selection-spatial manifold will also be analyzed via a tensor type of portraits. In our method, instead of utilizing vector stacking approach that conveniently concatenates special function vectors, a characteristic-spatial image tensor is constructed.mBecause manifolds could have arbitrary curvature in one-of-a-kind regions, we routinely decide upon a number of neighbors for patches through tensor sparse representation. For the image patch p centered at (i, j), we assemble its feature-spatial tensor Fi, j   p×m×R.

Through casting the sparse prior and twin-geometric constraint on the coding method, we can represent Fi, j with the aid of a multiview characteristic dictionary Di, j   p×d that's composed by way of the d nearest neighbors subsets of the patch p situated at (i, j), to receive the sparse coefficients tensor Xi, j   d×m×R, as proven in Fig.4 (b). According to the Tucker mannequin and Kronecker illustration of tensors discussed in section II.B, we now have Fi, j = Xi, j ×1 Di, j ×2 Im×m ×3 IR×R (7) given that very few patches are concerned in the sparse coding, Fi, j has a sparse representation with admire to the 1-mode dictionary Di, j   p×d. The 1-mode unfolding matrix can also be written as Fi, j (1) = Di, j(1) (Im×m   IR×R) and vec Fi, j=IR×R   Im×m   Di, Denote si, j as the number of atoms in synthesizing a HR patch for the patch p, the number of non-zero factors in vec Xi, j is si, jmR, i.E., vec Xi, j zero = si, jmR << dmR. Assuming there are Q patches, we are able to construct a brand new photo tensor F pQ×m×R and sparse coefficients tensor X
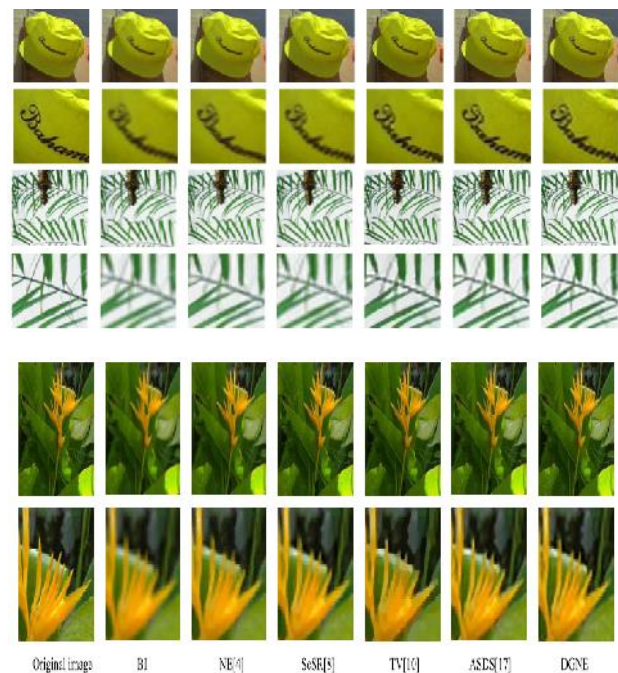
Fig.10. The LR image is divided into a set of LR patches,with an overlap of pixels between adjacent patches.

Firstlythe multiview features are extracted from the amplified LR patches (upsampled) via the six filters discussed in section II.A. Then the multiview feature set {fi } (i = 1, . . . , 6) ofpatches and their m spatial neighbors are combined as a feature-spatial image tensor F. The multiview 1-mode dictionaries composed by d candidate neighbors are constructed from the training examples, by which the image tensor F is sparsely coded. Tensor-SOMP algorithm is then used to calculate the sparse coefficients tensor X, which indicates the embedding neighbors and embedding weights.

As soon as the neighbors and coding coefficients are identified from the sparse tensors X, we can recover HR patches by weighting their sparse neighborhood patches.

Different with available NE-based SISR methods, the proposed DGNE cannot only combine heterogeneous multiview features together to better reveal the underlying manifold structure, but also jointly code spatial discrepancy patches to derive an accurate dual-geometric neighbors embedding. Moreover, tensor sparse coding will optimize the memory storage and require far fewer iterations compared to the traditional vector-based Orthogonal Matching Pursuit algorithm. For example, the vectorized form of the formula (9) can be written as, vec (F)=(IR×R   Im×m   D) vec X (10) In our method, the LR image is divided into a set of overlapping patches (denote the number of patches as Q and the image patch size as   p ×   p. If OMP is used to solve the sparse vec X, the computational complexity.

III. OBSERVATION & EXAMINED RESULTS

To validate the effectiveness of our proposed DGNE-based SISR algorithm, in this section 3 × magnification is conducted on eight LR natural images shown in Fig.6 [17], including humans, animals and plants. It is a popular benchmark dataset used for evaluating the available SISR methods. We use the software package in [8] to randomly generate 100,000 training pairs from 69 HR training images in this package. To produce the LR training images, all the training images are blurred by a 9 × 9 Gaussian kernel with standard deviation 1.1 and downsampled by a decimation factor of 3. In our experiment, the size of LR patch is 3 × 3 (upsampled to 6 × 6) with an overlap of two pixels between adjacent patches. The recovery results of DGNE are compared with that of Bicubic Interpolation (BI) and several examples-based and regularization-based SISR approaches, including NE [4], ScSR [8], TV-based method [10], SpNE [5], and ASDS [17]. We evaluate the results of various methods both visually and qualitatively, in terms of peak signal-to-noise ratio (PSNR), structural similarity (SSIM) [33]–[34], and feature similarity (FSIM) .
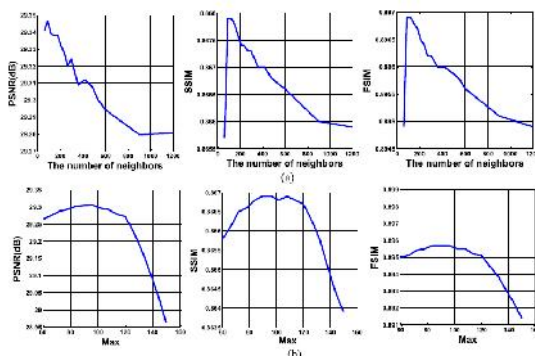

Fig. 11.   Performance of DGNE with different d and max.

Fig11: Investigation of the Multiview facets on this experiment we firstly investigate the superiority of multiview elements to a single feature. Taking a 6 × 6 snapshot patch in Fig.7 as an instance, we evaluate the 5 nearest neighbors discovered through more than a few facets when d = 1200, m = 1, max = a hundred,   = zero.1. Fig.7 (a) suggests the patches discovered by means of the primary-order and 2nd-order gradient characteristic, and Fig.7 (b) indicates the patches observed by using the first-order, 2nd-order gradient and PD function. Fig.7 (c) indicates the patches located by using the primary-order, 2d-order gradient and LG characteristic and Fig.7 (d) show the patches located through the primary-order, 2d-order gradient,PD and LG points. From Fig.7 (a) we will see that the nearest neighbor patches are very distinct with the patch, when you consider that the first-order and 2nd-order gradient features cannot well reflect the patch constitution. PD and LG facets can aid to find more an identical neighbor patches to the patch, as proven in Fig.7 (b) and Fig.7 (c) respectively. Fig.7 (d) plots the neighbor patches determined through the six multiview points. From it we can see that multiview aspects are extra risk-free to find neighbors, and hence bettering the recovery results of single view feature. Fig.Eight   (a),(b),(c),(d)   suggests   the   reconstructed photographs making use of exceptional facets in Fig.7 (a),(b),(c),(d) respectively. For the difference of neighbors found through one of a kind elements, the recovered graphics are one of a kind in important points. When put next with the recovered snap shots in Fig.Eight (a),(b),(c) that use elements in Fig.7 (a),(b),(c) respectively, the multiview aspects in Fig.7 (d) can in finding rather accurate neighbors, so leading to the smallest bias to the photo reconstruction, as proven in Fig.8 (d). To be able to investigate the performance of multiview features on extra graphics, we calculate the nearby keeping Ratio (NPR) [21] of various facets. Much like [24], we randomly prefer 5000 LR picture patches from the scan Eight photos. The traditional result of 20 trials is calculated and shown in Fig.9, when one-of-a-kind number of neighbors is considered. From it we are able to see that our developed multiview points remarkably outperform the single function, together with LG, PD and illuminance feature. Moreover, it is also sophisticated to the Gradients characteristic in NE [4], the Gradients + PD [8] characteristic and the Gradients + LG feature, for its better protection of nearby relationship through an exploration of complementary expertise of designated points B. Scan 2: Investigation of the tremendous-decision results The reconstructed graphics of exceptional SISR methods are shown in Fig.10, together with the amplified results of their local regions. Within the determine, the left column shows the customary graphics, and from left to proper the reconstructed pix through BI, NE [4], ScSR [8], television [10], ASDS [17] and our proposed DGNE methods respectively. The parameter of DGNE is set as d = 1200, m =

9, max = a hundred,   = zero.1. The parameters of comparative approaches are tuned to present fine outcome according to the urged surroundings in the references. From Fig.10 we will see that BI produces the worst results with blurred edges and jagging artifacts. NE [4] can partially get well excessive frequency accessories of portraits, but produce ringing effects alongside edges, for the participation of inaccurate neighbors within the reconstruction. ScSR [8] has a quite rapid attention, nevertheless it additionally generates blurred results on the grounds that of making use of too compact dictionary pairs. The television-based system [10] can significantly suppress the ringing results, nevertheless, it also generates obvious jaggy artifacts and smoothing details in the textural areas. The ASDS [17] method can good get better image details than the opposite methods as a result of its mixed regularization priors, with a slight bias to the long-established pix in element. Through exploring both the multiview characteristics and the spatial similarity among the neighborhood neighbors, DGNE can in finding extra correct neighbors and aid to provide richer details within the synthesized HR patch. Therefore, our proposed DGNE procedure outperforms NE [4], ScSR [8], tv [10], and is similar to ASDS [17]. From Fig.10 we will see that the recovered photos via DGNE are very constant with the usual snapshot, which is advanced to lots of the comparative approaches. It can be observed that there are tremendous variations between the reconstructed photos of DGNE and that of the other approaches, such because the black stripe close the eye of the parrot, the perimeters of the plant, and the direction of the crimple of the racer. Furthermore, DGNE also has some advantages over ASDS in small print, for example, in the reconstructed Bike pix, the cut down left corner of the bike appears a number of of vertical textures within the influence of ASDS, even as the textures are horizontal in the equal situation of the customary one. Within the reconstructed Hat picture by means of DGNE, the shape of the character 'B' is more similar to the fashioned photograph than that of ASDS. Desk II suggests the ordinary PSNRs (in decibels), SSIMs, and FSIMs of the reconstructed photos of one-of-a-kind ways through performing ten impartial checks. From the numerical outcome in desk II we will become aware of the prevalence of our process to NE [4], ScSR [8], television [10] and SpNE [5]. The results of ASDS are higher than DGNE on some snap shots, nonetheless, DGNE does now not utilize any regularizers at the same time ASDS employed two forms of adaptive legislation phrases to toughen results and the model of ASDS is more problematic. DGNE is related to ASDS on the normal outcome of the eight test pictures in phrases of PSNR, SSIM and FSIM. Furthermore, we evaluate the dual-geometric neighbor embedding with the Single-Geometric Neighbor Embedding (SGNE) in which the spatial geometric information shouldn't be used. From the influence we can see that DGNE is sophisticated to SGNE, for the exploration of

the self-similarity of pictures in the embedding. Nevertheless, DGNE is reasonably not as good as ASDS in terms of SSIM and FSIM for some pics, which is in general due to that we have now now not utilized any regularizers on the recuperation of the entire image. ASDS employs two types of adaptive regularization phrases to improve the restoration results, the place the global structural similarity is cast on portraits. So the 2 metrics on evaluating the global structural similarity and feature similarity between the recovered and fashioned photos, SSIM and FSIM, are higher than DGNE. C. Scan three: Investigation of the Parameter in DGNE within the proposed DGNE approach, there are three valuable parameters to be decided: the quantity of neighbors d, the quantity of spatial neighbors m, and the quantity of maximum iterations max in T-SOMP. In this experiment we to begin with investigate the have an impact on of d and max on the performance of DGNE on the eight graphics when m = 9. The typical outcomes of eight photos within the experiment 2 is calculated. Fig.11 (a) plot the averagPSNR, SSIM and FSIM of the recovered snap shots with the version of d when max = 100, from which we can see that when the quantity of neighbors is higher than one thousand, the recovered results are stable without super versions, so we set d = 1200 within the scan. Fig.Eleven (b) plot the average PSNR, SSIM and FSIM of the recovered Through exploring each the multiview characteristics and the spatial similarity among the many regional neighbors, DGNE can to find more accurate neighbors and aid to produce richer important points in the synthesized HR patch. As a result, our proposed DGNE strategy outperforms NE [4], ScSR [8], television [10], and is comparable to ASDS [17]. From Fig.10 we are able to see that the recovered graphics by DGNE are very regular with the normal photo, which is advanced to lots of the comparative methods. It can be located that there are amazing variations between the reconstructed pics of DGNE and that of the other approaches, such because the black stripe close the eye of the parrot, the perimeters of the plant, and the path of the crimple of the racer. In addition, DGNE also has some advantages over ASDS in details, for example, in the reconstructed Bike graphics, the lower left nook of the bike seems just a few of vertical textures within the influence of ASDS, at the same time the textures are horizontal in the same position of the normal one. Within the reconstructed Hat photo through DGNE, the form of the personality 'B' is extra much like the normal snapshot than that of ASDS. Desk II shows the usual PSNRs (in decibels), SSIMs, and FSIMs of the reconstructed graphics of special methods with the aid of performing ten unbiased checks. From the numerical results in table II we are able to realize the superiority of our system to NE [4], ScSR [8], tv [10] and SpNE [5]. The outcome of ASDS are better than DGNE on some snap shots, nonetheless, DGNE does now not make use of any regularizers even as ASDS

employed two varieties of adaptive regulation terms to beef up results and the model of ASDS is extra problematic. DGNE is comparable to ASDS on the typical result of the eight test pics in phrases of PSNR, SSIM and FSIM. Furthermore, we evaluate the twin-geometric neighbor embedding with the Single-Geometric Neighbor Embedding (SGNE) wherein the spatial geometric information shouldn't be used. From the effect we can see that DGNE is superior to SGNE, for the exploration of the self-similarity of pics within the embedding.

IV. CONCLUSION

From the Obsereved Editions, so we set d = 1200 within the test plot the common PSNR, SSIM and FSIM of the recovered portraits with the variation of max when d = 600, from which we can see that DGNE can present relatively steady results when max   [80, 120], so we set max = one hundred in the experiment. Then we set d = 600, max = one hundred, and examine the have an effect on of m on the recuperation result of DGNE. Three forms of spatial neighbors: 3×3, 5×5, 7×7 rectangular home windows are considered, when m = 9, 25, forty nine respectively. The typical outcome of eight pictures in scan 2 are proven in desk III. From it we will see that a small m can attain higher healing. In this paper, we recommend a novel twin-Geometric Neighbor Embedding (DGNE) procedure by exploring the geometric structure in each the characteristic area and spatial area. Multiview elements of snapshot patches and their spatial neighbors are jointly sparsely coded, through a tensor-simultaneous orthogonal matching pursuit algorithm. DGNE is attribute of easy precept for it does not introduce any additional regularizers in the restoration, which is one of a kind with most of the modern SISR strategies. Furthermore, it's also characteristic of viable attention for advancing a tensor SOMP to robotically select embedded neighbors. Some experiments are taken on some benchmark photographs, and the recovered outcome indicate that DGNE is similar to some latest SISR approaches without further regularizers. Additionally, both the multiview feature and local spatial neighbors of patches can support to search out extra accurate embedding.

REFERENCES

[1] A. Marquinaand and S. J. Osher, "Image super-resolution by TV-regularization and Bregman iteration," J. Sci. Comput., vol. 37, no. 3, pp. 367–382, Dec. 2008.

[2] S. Yang, Z. Liu, M. Wang, F. Sun, and L. Jiao, "Multitask dictionary learning and sparse representation based single-image super-resolution reconstruction," Neurocomputing, vol. 74, no. 17, pp. 3193–3203, 2011.

[3] Y. Tang, Y. Yuan, P. Yan, and X. Li, "Single-image super-resolution via sparse coding regression," in Proc. IEEE Int. Conf. Image Graphics,Aug. 2011, pp. 267–272.

[4] K. I. Kim and Y. Kwon, "Single-image super-resolution using sparse regression and natural image prior," IEEE Trans. Pattern Anal. Mach.Intell., vol. 32, no. 6, pp. 1127–1133, Jun. 2010.

[5] D. Glasner, S. Bagon, and M. Irani, "Super-resolution from a single image," in Proc. IEEE Int. Conf. Comput. Vision, Sep./Oct. 2009,pp. 349–356.

[6] K. Zhang, X. Gao, D. Tao, and X. Li, "Single image super-resolution with multiscale similarity learning," IEEE Trans. Neural Netw. Learn.Syst., vol. 24, no. 10, pp. 1648–1659, Oct. 2013.

[7] X. Gao, K. Zhang, X. Li, and D. Tao, "Joint learning for single-image super-resolution via a coupled constraint," IEEE Trans. Image Process., vol. 21, no. 2, pp. 469–480, Feb. 2012.

[8] W. Dong, D. Zhang, G. Shi, and X. Wu, "Image deblurring and super-resolution by adaptive sparse domain selection and adaptive regularization," IEEE Trans. Image Process., vol. 20, no. 7, pp. 1838–1857, Jul. 2011.